Published in final edited form as:
Cell Host Microbe. 2012 February 16; 11(2): 140–152. doi:10.1016/j.chom.2011.12.006.

Fatty Acid Synthase Modulates Intestinal Barrier Function through Palmitoylation of Mucin 2

Xiaochao Wei[1,6], **Zhen Yang**[1,6], **Federico E. Rey**[2,5], **Vanessa K. Ridaura**[2,5], **Nicholas O. Davidson**[1,3], **Jeffrey I. Gordon**[2,5], and **Clay F. Semenkovich**[1,4,*]

[1]Department of Medicine, Washington University School of Medicine, St. Louis, MO 63110

[2]Department of Pathology and Immunology, Washington University School of Medicine, St. Louis, MO 63110

[3]Department of Developmental Biology, Washington University School of Medicine, St. Louis, MO 63110

[4]Department of Cell Biology and Physiology, Washington University School of Medicine, St. Louis, MO 63110

[5]Center for Genome Sciences and Systems Biology, Washington University School of Medicine, St. Louis, MO 63110

SUMMARY

The intestinal mucus barrier prevents pathogen invasion and maintains host-microbiota homeostasis. We show that fatty acid synthase (FAS), an insulin-responsive enzyme essential for de novo lipogenesis, helps maintain the mucus barrier by regulating Mucin 2, the dominant mucin in the colon and a central component of mucus. Inducible Cre recombinase-directed inactivation of the FAS gene in the colonic epithelium of mice is associated with disruptions in the intestinal mucus barrier as well as increased intestinal permeability, colitis, systemic inflammation, and changes in gut microbial ecology. FAS deficiency blocked the generation of palmitoylated Mucin 2, which must be S-palmitoylated at its N-terminus for proper secretion and function. Furthermore, a diabetic mouse model exhibited lower FAS levels and a decreased mucus layer, which could be restored with insulin treatment. Thus, the role of FAS in maintaining intestinal barrier function may explain the pathogenesis of intestinal inflammation in diabetes and other disorders.

INTRODUCTION

Critical functions such as programming of the immune system and processing of nutrients are impacted by the commensal relationship between a mammalian host and its intestinal microbiota (Kau et al., 2011; Macpherson and Harris, 2004). This relationship is predicated on the ability of the host to restrict bacteria to the lumen of the intestine. Separation of host and bacteria depends on humoral and physical barriers. The former consists of IgA, α-defensins, lysozymes, lectins such as RegIIIγ (Vaishnava et al., 2011), and other

*Correspondence: csemenko@wustl.edu.
[6]Contributed equally to this work.

antimicrobial factors (McGuckin et al., 2011). The latter consists of the intestinal epithelium and its overlying mucus, a component of which is normally sterile (Johansson et al., 2008). The relationship between the mucus barrier and the microbiota is dynamic. Goblet cells, the source of mucus, are decreased in germfree mice (Kandori et al., 1996), genes involved in mucus secretion are regulated by the microbiota (Comelli et al., 2008), and products of bacterial fermentation such as butyrate increase colonic mucus synthesis (Finnie et al., 1995). These observations indicate that the resident microbiota affects the biology of the mucus barrier.

Surprisingly, there is relatively little information regarding the effect of pathogens on the mucus barrier. Rotavirus infection in mice increases production of the most abundant gel-forming component of mucus, Mucin 2 (Muc2), and results in mucins capable of neutralizing rotavirus in vitro (Boshuizen et al., 2005). Also in mice, changes in mucus production and composition appear to facilitate clearance the parasites *G. seoi* (Guk et al., 2009) and *T. muris* (Hasnain et al., 2011). While our understanding of the impact of pathogens on the mucus barrier during infection is limited, even less is known about how factors intrinsic to the host may affect the integrity of the mucus barrier and promote infection.

One host factor important for the maintaining homeostasis in several tissues is de novo lipogenesis, which involves the conversion of simple precursors into fat. In mammals, this process requires fatty acid synthase (FAS), a multifunctional protein that synthesizes saturated fatty acids for cell membranes, energy stores, and signaling molecules (Lodhi et al., 2011; Wakil, 1989). FAS expression is induced by insulin, in part through transcriptional mechanisms that include SREBP-1c and LXRα (Wong and Sul, 2010). Diabetes is frequently associated with gastrointestinal complications (Sellin and Chang, 2008), including increased gut permeability reflecting colonic as well as small intestinal abnormalities (Bosi et al., 2006; Meddings et al., 1999). Mechanisms underlying these abnormalities and the effects of the diabetic state on interactions between the human gut microbiota and host remain poorly understood.

Increased epithelial permeability can precede the development of chronic intestinal inflammation (Olson et al., 2006). Serum levels of endotoxin are elevated in humans with both type 1 and type 2 diabetes (Creely et al., 2007; Devaraj et al., 2009) suggesting disruption of homeostasis that normally exists between the microbiota and host and that is required for maintaining gut integrity. Host-microbial interactions in the gut, in turn, can be markedly impacted by the loss of integrity of the mucosal barrier (Garrett et al., 2010). To understand how gut lipogenesis affects intestinal physiology, including barrier function, we used an inducible Cre recombinase driven by the intestine-specific villin promoter to inactivate FAS in the gut epithelium of 6–8 week old mice.

RESULTS

Intestinal FAS Deficiency Initiates Inflammation

Tamoxifen induction of Cre recombinase for 5 days decreased intestinal FAS protein, mRNA, and tissue staining in adult (6–8 week old) mice hemizygous for the Cre transgene and homozygous for the floxed FAS allele (Villin-Cre-ER:$FAS^{f/f}$; abbreviated FAS-villin) but not in control mice homozygous for the floxed allele but lacking the Cre transgene ($FAS^{f/f}$) (Fig. 1A, B). Decreased FAS expression was noted along the length of the intestine, but was most prominent in the distal small intestine and colon, where FAS expression is normally highest (Fig. 1B, C). Intestinal FAS expression was unaffected in vehicle-treated FAS-villin mice. Moreover, no diminution in FAS was noted in the liver, fat, lung, brain, or spleen of tamoxifen-treated FAS-villin compared to control mice (Fig. 1A, right panels).

Tamoxifen-induced deletion of intestinal FAS in FAS-villin mice was associated with a statistically significant decrement in body weight that did not occur in (i) FAS-villin mice treated with vehicle alone, (ii) Cre transgenic mice without the floxed FAS allele treated with tamoxifen, (iii) FAS floxed mice without the Cre transgene treated with vehicle, or (iv) FAS floxed mice without the Cre transgene treated with tamoxifen (Fig. 2A). This weight loss was evident after 5 days of tamoxifen treatment, progressed over the ensuing 9 days, and then slowly resolved, a time course mirroring the normal period required to a complete a cycle of epithelial renewal. Weight loss was associated with statistically significant decreases in adipose tissue, food intake (Fig. S1A–C), fasting serum glucose, triglycerides and free fatty acids (Fig. S1D–F). 20% of FAS-villin animals died within 14 days after induction of Cre expression compared to none in all of the control groups (n=46 and 48 animals, respectively; Fig. 2B).

Imaging live mice after oral administration of labeled dextran revealed that deletion of FAS resulted in disruption of intestinal barrier integrity: fluorescence in the intestinal lumen was diminished (due to increased absorption of the usually impermeable tracer) in FAS villin mice as compared to controls ($P<0.01$; t-test; n=12 FAS floxed controls and 14 FAS-villin mice; Fig. 2C). In a confirmatory assay, circulating concentrations of FITC-labeled dextran (both 4 kDa and 40 kDa species in independent experiments) after gavage were significantly higher in FAS-villin animals ($p<0.01$; t-test; n=13 control and 9 FAS-villin for FD4 [FITC dextran 4 kDa]; n=15 control and 12 FAS-villin for FD40 [FITC dextran 40 kDa]; Fig. S2A,B). Consistent with increased access of intestinal contents to the systemic circulation, serum levels of TNFα, endotoxin, and LBP (lipopolysaccharide binding protein) were elevated in FAS villin mice (Fig. 2D–F).

The macroscopic appearance of large intestinal contents was altered (Fig. S2C) and fecal wet/dry ratio was increased ($P<0.01$; t-test; n=7 control and 12 FAS-villin; Fig. S2D), suggesting a diarrheal syndrome in FAS-villin mice. There was loss of crypts in the ileum and cecum of FAS-villin mice (quantified in Fig. S2E). Tissue ELISA assays showed statistically significant increases in TNFα and IL-1β in the colons of FAS-villin animals (Fig. 2G). MPO activity was significantly increased in FAS-villin colon (Fig. 2H). The FAS-villin colonic lamina propria was infiltrated with more significantly more mononuclear cells as determined by FACS (Fig. S2F); these results were confirmed by CD11b and MOMA staining (not shown, n=3–4 animals per condition). Blinded histological scores demonstrated significantly increased inflammation in the cecum (Fig. 2I). The same trend was observed in the colon (Fig. S2G). *tnfα* expression was increased in the distal small intestine but other biomarkers of inflammation were not (data not shown). Apoptosis, detected by TUNEL staining (Fig. S2H) and confirmed by caspase-3 staining (data not shown), was significantly increased in FAS-villin colon, as was proliferation (detected by Ki67 staining, Fig. S2I, and BrdU, data not shown). β-catenin, part of the Wnt signaling pathway intimately involved in epithelial barrier function and intestinal proliferation, was activated to a greater extent in FAS-villin colon (data not shown). These findings suggest a hyperplastic response characteristic of repair following injury to the mucosal barrier (van der Flier and Clevers, 2009).

FAS-villin Microbiota Fail to Transfer the Inflammatory Phenotype to Germ-free Mice

Pyrosequencing variable region 2 (V2) of bacterial 16S rRNA genes present in the cecal microbiota harvested from conventionally raised, tamoxifen-treated, FAS-villin and control mice consuming a standard polysaccharide-rich, low fat chow diet (n=5–7 animals/group; 2419±495 reads/sample; Table S1) disclosed that loss of FAS did not have a statistically significant effect on alpha diversity (overall richness as measured using the Chao1 estimator and observed number of species-level phylotypes). Beta-diversity analyses (between sample comparisons) revealed that loss of FAS was accompanied by modest albeit statistically

significant differences in the representation of class level taxa belonging the Firmicutes, Bacteroidetes and Proteobacteria phyla (Table S1). Principal coordinates analysis (PCoA) based on pairwise comparisons of UniFrac distances between fecal bacterial communities failed to show significant clustering based on host genotype (UniFrac measures the overall degree of phylogenetic relatedness of communities based on the degree to which they share branch length on a bacterial tree of life). Differences in class-level taxonomic representation were not maintained when cecal microbiota from FAS-villin mice and control animals were transplanted into 8-week old wild-type germ-free C57BL/6J recipients for 2 weeks (n=6 mice/group; 1158 ± 674 denoised V2 16S rRNA reads/sample).

Furthermore, transplantation of cecal microbiota pooled from multiple FAS-villin or control donors into multiple adult germ-free wild-type C57BL/6J mice resulted in no differences in body weights, body composition, or intestinal histology between the two groups of recipient animals at the end of the 2-week interval (Fig. 3A–C). Together, these findings suggest that changes in gut microbial ecology accompanying conditional FAS gene knockout in the distal intestinal epithelium were a response to, rather than a cause of, observed changes in the structure and function of the mucosal barrier.

Antibiotic Treatment Ameliorates the Inflammatory Phenotype of FAS-villin Mice

Administration of ciprofloxacin (9.9 mg/kg) and metronidazole (37.5 mg/kg) by daily oral gavage beginning at the time of tamoxifen induction of Cre expression resulted in significantly less weight loss in FAS-villin as compared to control mice (Fig. 3D). Antibiotic treatment corrected the increased wet/dry ratio of feces (Fig. 3E), normalized serum endotoxin (Fig. 3F), and significantly decreased serum TNFα concentrations (Fig. 3G) in FAS-villin mice. These findings suggest that the gut microbiota contributes to the inflammatory state induced by FAS depletion.

Intestinal FAS Deficiency Decreases Muc2 and Disrupts the Inner Mucus Layer

One interpretation of these results is that the FAS-villin phenotype is caused by a cell autonomous process operating at the level of the intestinal epithelium. While the number of enteroendocrine cells and absorptive enterocytes (detected by chromogranin A and alkaline phosphatase staining, respectively, Fig. 4A, B) were minimally affected in the colons of FAS-villin animals, alcian blue staining for mucus was dramatically decreased, suggesting a defect in the third colonic epithelial lineage, namely, mucin-producing goblet cells (Fig. 4C).

The mucus blanket overlying the intestinal epithelium consists of an inner stratified layer that is tightly adherent to epithelial cells and an outer unattached layer. These two layers are organized into a net-like polymer around Mucin2 (Muc2), the most abundant mucin protein, which is heavily glycosylated and secreted by goblet cells (Johansson et al., 2011). Mucus thickness varies along the length of the gut, is greatest in the colon (Johansson et al., 2011), and is modulated by the microbiota (Comelli et al., 2008).

Muc2 levels were decreased in the colons of FAS-villin versus control mice, as assessed by immunocytochemistry (Fig. 4D). Colonic Muc2 mRNA levels were also significantly lower in FAS-villin mice ($P<0.05$, t-test; n=5 animals per group; Fig. 4E). Expression of another secreted goblet cell protein associated with the mucosa, trefoil factor 3 (Tff3), was not significantly different between FAS conditional knockout mice and controls (Fig. 4F), suggesting that loss of FAS produced selective defects in protein secretion by this epithelial lineage. Decreased Muc2 expression was associated with a significant decrease in the average thickness of the inner stratified mucus layer in the colons of fasted FAS-villin as compared to fasted control mice (Fig. 4G, H). Dual label immunocytochemistry using a

Muc2 antibody and the lectin Dolichos Biflorus Agglutinin (DBA; carbohydrate specificity alpha-linked N-acetylgalactosamine) that recognizes Muc2 due to its extensive O-glycosylation (Johansson et al., 2008) further confirmed loss of normal Muc2 in FAS-villin mice (Fig. 4I). CEACAM1, a pleotropic adhesion molecule involved in epithelial function and immunity, is found in Muc2-containing mucus layers (Johansson et al., 2008) and has been implicated in regulation of FAS (Najjar et al., 2005). *Ceacam1* expression was decreased in the colon (by ~30%) and ileum (by ~45%) of FAS-villin mice compared to control mice (each $P<0.05$; two-tailed unpaired t-test; n=4 control and n=5 FAS-villin).

FAS is Required for Normal Muc2 Secretion

To identify a potential molecular link between FAS and mucin biogenesis, we replicated the effect of FAS deficiency on Muc2 in cultured cells. Muc2 protein was significantly decreased in extracts prepared from colons of FAS-villin mice (Fig. 5A), and decreased among the proteins secreted from LS174T cells (a colon carcinoma cell line) after lentivirus-mediated shRNA knockdown of FAS (Fig. 5B). Since the Muc2 N-terminus is involved in its secretion (Godl et al., 2002), we expressed the HA-tagged N-terminus of Muc2 (N-Muc2; residues 1–300) in COS cells. Little is known about the structural domains required for normal secretion of Muc2, but using our expression system in these cells, an intact protein of the expected size (~38 kDa) as well as a band likely representing a dimer (~76 kDa) were detected in cell lysates (Fig. 5C). Only the dimer was detected in supernatants indicating secretion of this form. No shorter fragments were detected with the anti-HA antibody and there was no evidence of cell death or lysis as judged by morphology.

Knockdown of FAS expression in N-Muc2-expressing cells impaired N-Muc2 secretion (Fig. 5C; note the decrease in dimeric N-Muc2 in the supernatant fraction of FAS knockdown cells). Conversely, overexpression of FAS in the COS cells increased N-Muc2 secretion (Fig. 5D). Thus, FAS appears to be involved in Muc2 secretion and this effect can be modeled in cultured cells.

The major product of FAS is palmitate, which is converted to palmitoyl-CoA, the substrate for DHHC palmitoyl transferases. These membrane-associated transferases catalyze the reversible post-translational linkage of palmitate via a thioester bond to cysteines on a variety of proteins (Greaves and Chamberlain, 2011). FAS from silkworms can carry out S-palmitoylation of synthetic peptides (Ueno and Suzuki, 1997), and FAS is involved in Wnt-1 S-palmitoylation in prostate cancer cells (Fiorentino et al., 2008) as well as eNOS S-palmitoylation in endothelial cells (Wei et al., 2011). To determine if the Muc2 N-terminus is S-palmitoylated, COS cells transfected with N-Muc2 were subjected to a biotin switch assay for S-palmitoylation (Wan et al., 2007). With this technique, free thiols are chemically blocked with N-ethylmaleimide, hydroxylamine is used to cleave thioester bonds at palmitoylation sites, these sites are biotinylated, and the biotinylated protein is affinity-captured and detected by Western blotting. N-Muc2 showed a hydroxylamine-dependent signal in the biotin switch assay (Fig. 5E), indicating S-palmitoylation. Sequence analysis of the Muc2 N-terminus revealed potential sites for S-palmitoylation: Cys12, Cys163, and Cys166 (Fig. 5F). When Cys12 was mutated to Ser (Fig. 5G, C12S), N-Muc2 dimer formation was blocked but the monomer was secreted normally (Fig. 5G, lower panel, compare C12S and Wt lanes). Mutation of Cys163 or Cys166 to Ser, or mutation of both residues to Ser abolished secretion (Fig. 5G). In palmitoylation assays, signal was diminished when either Cys163 or Cys166 was mutated to Ser (Fig. 5H, only C166S is shown) suggesting decreased palmitoylation. When both sites were mutated (C163S, C166S), N-Muc2 palmitoylation was essentially abolished (Fig. 5H). Note that the palmitoylation assay detects lipid modification in cell extracts, and that decreased S-palmitoylation due to loss of the thiol group at either Cys163 or Cys166 is capable of blocking protein secretion (Fig. 5G, H). S-palmitoylated N-Muc2 (detected in extracts

treated with hydroxylamine) is strikingly decreased when FAS was knocked down (Fig. 5I). In concert with our finding that FAS knockdown also impairs Muc2 secretion (Fig. 5B, C), these results suggest that FAS-dependent S-palmitoylation of Muc2 is required for its normal secretion.

Impaired Muc2 secretion induced by loss of FAS could be associated with ER stress. When assayed prior to the development of the systemic inflammatory phenotype, mRNAs for *XBP1s/u* and *CHOP* were significantly increased in mouse colon (Fig. S3A). FAS knockdown in LS174T cells was associated with significantly increased mRNA levels for *GRP78*, *CHOP*, and *XBP1s/u* (Fig. S3B), suggesting that ER stress might contribute to the inflammation of FAS-villin mice.

Since several tight junction proteins are S-palmitoylated, it is possible that part of the impaired barrier function phenotype is mediated by mucin-independent effects. There was no overt disruption of the tight junction proteins occludin and ZO-1 as judged by immunocytochemistry (n=3 mice per condition; Fig. S3C,D). Claudins are major functional determinants of the epithelial tight junction barrier, and palmitoylation of claudin-14 in a kidney cell line is required for its proper localization in tight junctions (Van Itallie et al., 2005). Claudin-1 protein levels were decreased in the colons of FAS-villin as compared to control mice as assessed by immunocytochemistry (n=3 mice per condition, Fig. S4A top); decreased claudin-1 protein staining was also seen in the colons of Muc2 deficient mice (n=3 mice per condition, Fig. S4A bottom). These findings are consistent with a recent report that claudin-1 mRNA is decreased in the colons of Muc2 knockout mice in the setting of colonic inflammation (Lu et al., 2011). However, when FAS was knocked down in Caco-2 cells, there was no major effect on claudin-1 S-palmitoylation as determined by the biotin-switch assay (Fig. S4B), and claudin-1 protein was not decreased as assessed by immunocytochemistry (Fig. S4C). Collectively, these results suggest that FAS deficiency does not affect claudin-1 S-palmitoylation or claudin protein directly, but may affect claudin-1 levels in colon in vivo due to chronic inflammation induced by disruption of Muc2 function.

Diabetic Mice have an Intestinal Phenotype Mimicking FAS-villin Mice

Since FAS is induced by insulin and the intestinal mucus layer is decreased in diabetic rodents (Igarashi et al., 2000), we assessed FAS expression in mice with experimental diabetes. Compared to relevant controls, colonic FAS protein content was significantly lower in two diabetes models: C57BL/6 mice treated with streptozotocin (STZ) and transgenic C57BL/6 mice with engineered expression of an ATP-insensitive K_{ATP} channel (Kir6.2) in pancreatic beta-cells (Remedi et al., 2009) (Fig. 6A). Circulating concentrations of FITC-labeled dextran after gavage (the same assay used to study FAS-villin mice, Fig. S2A) were significantly higher in STZ-treated animals (Fig. 6B). The average thickness of the inner stratified mucus layer was decreased in the colons of STZ-treated as compared to control mice (Fig. 6C,D), and the colonic epithelium of STZ-treated mice was infiltrated with more inflammatory cells as compared to controls (n=4 mice per condition; Fig. S4). These results demonstrate that intestinal barrier function is disrupted in experimental diabetes, mimicking effects seen in FAS-villin mice.

Analogous to FAS-villin mice, STZ-treated mice manifested decreased goblet cell staining. The inner mucus layer (Fig. 6E, arrow) was clearly identified in controls but not in STZ-treated mice, suggestive of a defect in Muc2 with insulin deficiency.

The inner, tightly adherent mucus layer prevents bacteria from accessing the epithelium (Johansson et al., 2011). Staining with a fluorescent probe for bacteria (Johansson et al., 2008) showed the presence of bacteria deep within the intestinal epithelium in FAS-villin

mice (arrows in Fig. 6F), while bacteria were limited to the lumen by the intact mucus gel layer in controls (3 mice surveyed/treatment group). The same stain in control and STZ-treated mice showed a discrete clear layer separating bacteria and mucosal epithelium in control mice (Fig. 6G, double-headed arrow on left): this layer was disrupted in STZ-treated mice and accompanied by the presence of bacteria deep within the epithelium (Fig. 6G, arrows). Disruption of the mucus barrier and penetration of bacteria into the epithelium in FAS-villin are consistent with increased intestinal permeability and increased circulating levels of TNFα, LPS, and LBP in these animals.

To determine if the increased permeability of mice with diabetes can be reversed by insulin, C57BL/6 mice were injected with STZ (Fig. 7A, day 0) to induce diabetes then implanted with pumps delivering either saline or insulin (Fig. 7A, day 3). Glucose levels in mice fed ad libitum (Fig. 7A) were significantly lower in those that were insulin-treated compared to saline-treated from days 4–12. Fasting glucose levels were also significantly decreased with insulin (data not shown). Of note, insulin therapy improved but did not normalize the glucose phenotype of the diabetic mice. At day 12, colonic FAS protein was decreased in saline-infused mice but increased in insulin-infused mice (Fig. 7B). Insulin treatment significantly increased body weight (Fig. 7C). As seen with another cohort of STZ-diabetic mice (Fig. 6D), diabetes decreased inner mucus layer thickness (Fig. 7D). Insulin treatment increased the thickness of this layer as shown in Fig. 7D ($p=0.05$). The results of alcian blue staining of colons from control non-diabetic, saline-infused diabetic, and insulin-infused diabetic mice are presented in Fig. 7E with the inner mucus layer denoted by arrows. Insulin treatment significantly decreased circulating FD4 (FITC dextran 4 kDa) in diabetic mice (Fig. 7F), and this value was not significantly different from controls, indicating that insulin corrected the permeability phenotype in this diabetes model.

DISCUSSION

Our findings suggest that the insulin-regulated enzyme FAS modifies mucosal barrier integrity in intestinal epithelial cells in part by affecting Muc2 lipidation and that this effect is accompanied by changes in mucosal barrier function. While we acknowledge that FAS could also be affecting other aspects of intestinal biology, our observation linking FAS and Muc2 identifies a potentially important element in the multifaceted regulation of the intestinal mucus layer (Johansson et al., 2011). FAS deficiency impaired Muc2 secretion and was associated with decreased goblet cell Muc2. FAS-villin mice bear a striking resemblance to mice with missense mutations in *Muc2* (Heazlewood et al., 2008). These mutations are also associated with decreased Muc2 in the setting of defective secretion, suggesting that accumulation of Muc2 might promote its degradation or accelerate goblet cell loss. Muc2 mutant mice, like FAS-villin mice, have a defective mucus barrier, increased intestinal permeability, enhanced inflammation, and colitis. Evidence of ER stress accompanies the phenotype in both models.

Mice genetically deficient in *Muc2* eventually develop colorectal cancers (Velcich et al., 2002): they are missing the inner adherent mucus layer and, as with FAS-villin mice, bacteria penetrate deep into the colonic epithelium of these animals (Johansson et al., 2008) to promote inflammation. Since intestinal FAS expression as well as mucus thickness is greatest in the colon, and FAS deficiency caused by genetic manipulation or insulin deficiency is associated with a defective inner mucus layer, the insulin-FAS-Muc2 axis appears to be critical for regulating the intestinal mucus barrier.

FAS expression is decreased in the ileum and colon of humans with ulcerative colitis (Heimerl et al., 2006). Evidence linking FAS and human inflammatory bowel disease is limited. Our findings in mice could prompt speculation that FAS-mediated effects on Muc2

might exacerbate inflammation in humans. Moreover, FAS is induced by insulin, and there are reports that hyperinsulinemia is associated with protection from clinical relapse in patients with inflammatory bowel disease (Valentini et al., 2009).

Diabetes as well as obesity and the metabolic syndrome might be impacted by the insulin-FAS-Muc2 axis in the intestine. The microbiota is involved in diabetes syndromes in mice (Vijay-Kumar et al., 2010; Wen et al., 2008), although alterations in microbial composition in metabolic disorders tend to be more pronounced than the effects we found with FAS deficiency. Diabetes and the metabolic syndrome represent chronic inflammatory states characterized by activation of systemic and cell-autonomous inflammatory pathways (Shoelson et al., 2006). It is not known if these pathways are modulated by FAS through its effects on host-microbial interactions in human diabetes syndromes. It is also not known if different microbial community structures can affect host FAS. However, our work raises the possibility that an alteration in the host, namely decreased barrier function due to altered FAS, facilitates microbial access to promote inflammation.

Both type 1 and type 2 diabetes require pancreatic beta cell dysfunction manifested as insufficient insulin secretion to control glucose metabolism. Colonic lymph drains to pancreatic lymph nodes in mice (Carter and Collins, 1974), suggesting a plausible framework to explain how disruption of intestinal FAS could contribute to the diabetic state. This notion is supported by recent data showing that endotoxemia, presumably due to increased intestinal permeability, is associated with the development of diabetes independent of risk factors such as obesity, lipids, and C-reactive protein (Pussinen et al., 2011).

In summary, the insulin-responsive enzyme FAS in intestinal epithelial cells affects mucosal barrier function in mice by lipidating Muc2. Considerable additional work will be required to implicate FAS modulation of host-microbial interactions in the pathophysiology of metabolic diseases. This may include identifying strategies that promote lipogenesis to preserve Muc2 acylation or that inhibit Muc2 deacylation. Testing the impact of these strategies in models characterized by mucosal barrier dysfunction and chronic inflammation could lead to novel therapies for diabetes syndromes.

EXPERIMENTAL PROCEDURES

Animal Models

The Washington University Animal Studies Committee approved protocols. Mice with inactivation of FAS in the intestine (FAS-villin mice) were generated by crossing floxed FAS mice (Chakravarthy et al., 2005) with villin-Cre-ER^{T2} mice (el Marjou et al., 2004). Littermates of mixed genetic background at 6–8 weeks of age were used for experiments that included administering tamoxifen (1 mg per mouse) or vehicle for five consecutive days as described (el Marjou et al., 2004). To induce diabetes, streptozotocin (150 mg/kg) or vehicle was administered to 2-month old C57BL/6J male mice, and diabetic animals were studied in the setting of a serum glucose >300 mg/dl one week later. Hyperglycemic mice carrying an ATP-insensitive mutant K_{ATP} channel in beta cells and control Rosa-Kir6.2 mice were a gift from Colin Nichols (Remedi et al., 2009). Muc2 null mice and wild type controls each in the C57BL/6J background were studied at 3 months of age.

Bacterial 16S rRNA Analyses and Microbiota Transplants

Details of methods and analysis for microbiota sequencing are provided in Supplemental Information. For microbiota transfer experiments, cecal contents were recovered from conventionally raised FAS-villin mice 9 days after initiation of a 5-day treatment period with tamoxifen or vehicle. Methods for gavage of harvested communities into germ-free 8 week-old C57BL/6J mice (n=6 donor samples pooled from the control group and n=9 donor

samples pooled from FAS-villin mice; each pooled sample introduced into 6 recipients) are described (Turnbaugh et al., 2006). All donors and all recipients were fed the same plant polysaccharide-rich/low fat chow diet (B&K Universal, Ltd). Fourteen days after transplant, recipient gnotobiotic mice were subjected to the phenotypic assays described in the main text, then sacrificed and their cecal contents removed for 16S rRNA-based analyses.

Intestinal Permeability Assays

Mice were gavaged with dextran (4 kDa or 40 kDa) conjugated to *fluorescein* isothiocyanate (Sigma), then sacrificed four h later and their serum was collected for fluorescence measurements (490 nm excitation/520 nm emission). Fluorescence detection in living, anesthetized mice was captured with a Carestream In-Vivo Imaging System FX Pro system (Kodak). Fluorescent conjugated dextran (10 kDa with Alexa Fluor 680) was gavaged into mice, and thenanimals were studied 1 h later using multispectral fluorescent capture (450 nm to 630 nm excitation with 700 nm emission) followed by digital X-ray imaging. Nonspecific background signals were removed, and mice not subjected to gavage were included in experimental runs. The fluorescent intensity of the dye after gavage was calculated using software provided by the manufacturer and the results corrected by subtraction of signal measured in mice not subjected to gavage.

Cytokine ELISA and Myeloperoxidase Activity Assay

Colons were flushed with PBS to remove luminal contents, opened and washed three times by gentle agitation in HBSS with antibiotics (15 minutes for each wash), then minced into small pieces and transferred to 24-well plates with growth media containing antibiotics. After a 24-h incubation, the supernatants were collected and subjected to ELISAs for several cytokines according to the instructions provided by the manufacturer (TNFα and Interferon γ, BD Bioscience; IL-17, IL-1β, and IL12p40, R&D Systems).

For the myeloperoxidase activity assay, tissues were homogenized in a solution of 0.5% hexadecyltrimethyl ammonium bromide in 50 mM potassium phosphate buffer (pH 6.0), subjected to three rapid freeze-thaw cycles, and then centrifuged at 4° C to remove insoluble material. The MPO containing supernatant (0.1 ml) was assayed after addition of 2.88 ml phosphate buffer containing 0.167 mg/ml *o*-dianisidine hydrochloride (Sigma) and 0.0005% hydrogen peroxide. The kinetics of absorbance changes at 450 nm (37° C) were measured as MPO activity and results were normalized by protein concentrations.

Histological Scoring

Hematoxylin and eosin stained slides were scored by observers unaware of the animal genotype based on a known assessment system (Rachmilewitz et al., 2002) as follows: A. Depth/degree of ulcer: 0-no ulcer; 1-mucosal involvement; 2-mucosal-submucosal involvement; 3-invasion of the muscularis propria; 4-full thickness penetration. B. Extent of ulcer: 0-no ulcer; 1-punctate, <10%; 2-minimal, 10–25%; 3-moderate, 26–50%; 4-widespread, >50%. C. Degree of inflammation: 0-none; 1-mucosal, increased cellularity between crypts, crypt almost normal; 2-mucosal + submucosal involvement, moderate cellullar increase, distorted crypts <50%; 3-mucosa+submucosal +inflammatory infiltrate in the muscularis propria, large increase in cellularity, distorted crypts >50%; 4-full thickness involvement, loss of all crypts. D. Extent of inflammation (fraction of the width of a single 10X field): 0-none; 1-minimal, <25%; 2-mild, 25–50%; 3-moderate, 51–75%; 4-severe, >75%. E. Degree of edema (width of the clear space in the muscularis mucosa): 0-none; 1-minimal, width <1x; 2-mild, 1–2x; 3-moderate, >2–3x; 4-severe, >3x. F. Extent of edema: 0-none; 1-minimal, <25%; 2-mild, 25–50%; 3-moderate, 51–75%; 4-severe, >75%.

FACS Analysis

Colons were isolated and washed as described above for ELISA assays. Cell suspensions from the lamina propria were obtained by mincing tissues into small pieces, followed by digestion using collagenase (1 mg/ml, Worthington), dispase I (1 mg/ml, Invitrogen) and DNase I (50 μg/ml, Roche). After red blood cell lysis using an RBC lysis buffer (eBioscience), filtered cells were counted and identified by FACS using antibodies (eBioscience) against CD11b and F/80 (PE, BM8).

Assays for Protein S-Palmitoylation

A biotin switch assay (Wan et al., 2007) was modified to detect S-acylation of Muc2. Cells were homogenized in lysis buffer [150 mM NaCl, 50 mM Tris (pH 7.4), 5 mM EDTA] in the presence of 20 mM NEM, sonicated on ice, then Triton-X-100 (1.7%) was added and the mixture was rotated in a cold room. Samples were treated with chloroform/methanol (1:4), solubilized in 4% SDS with 20 mM NEM at 37°C for 3 h, and subjected to serial protein precipitations to remove residual NEM. Each sample was then aliquoted to two tubes and resuspended in buffer containing HPDP-biotin (1 mM) and Triton X-100 (0.2%) in the presence or absence of hydroxylamine (NH_2OH). After 1 h, proteins were precipitated twice with chloroform/methanol, solubilized in buffer containing 0.1% SDS, streptavidin-agarose beads were added, the mixture was incubated for 1.5 h at room temperature, then biotin-labeled proteins were detected by Western blotting.

Insulin Treatment of Diabetic Mice

Following administration of streptozotocin (STZ, 150 mg/kg) or vehicle as described above in 2-month old C57BL/6 male mice, diabetic animals were implanted with micro-osmotic pumps (Alzet, model 1004) containing either saline or insulin (5 mU per kg of body weight per day). Mice were divided into 3 groups: vehicle injection (non-diabetic control group); STZ injection with implantation of pump infusing a saline solution; and STZ injection with implantation of pump infusing an insulin solution.

Statistics

Data are expressed as mean ± SEM except as indicated. The two-tailed unpaired t-test was used for most comparisons except for survival curves that were compared using the logrank test.

Details of methods used for histology and immunohistology, serum assays, quantitative RT-PCR, Muc2 manipulations, and generating and analyzing metagenomic (bacterial 16S rRNA) datasets are provided in Supplemental Information.

Supplementary Material

Refer to Web version on PubMed Central for supplementary material.

Acknowledgments

We thank Li Yin, Trey Coleman, and Yan Xie for technical expertise, and Maria Karlsson and David O'Donnell for assistance with gnotobiotic mouse experiments. This work was supported by NIH grants DK076729, DK088083, DK20579, DK56341, DK52574, DK56260, HL38180, and DK70977, by the American Heart Association (Postdoctoral Fellowship Award), and by the American Diabetes Association (Mentor-Based Postdoctoral Fellowship Award).

References

Boshuizen JA, Reimerink JH, Korteland-van Male AM, van Ham VJ, Bouma J, Gerwig GJ, Koopmans MP, Buller HA, Dekker J, Einerhand AW. Homeostasis and function of goblet cells during rotavirus infection in mice. Virology. 2005; 337:210–221. [PubMed: 15882887]

Bosi E, Molteni L, Radaelli MG, Folini L, Fermo I, Bazzigaluppi E, Piemonti L, Pastore MR, Paroni R. Increased intestinal permeability precedes clinical onset of type 1 diabetes. Diabetologia. 2006; 49:2824–2827. [PubMed: 17028899]

Carter PB, Collins FM. The route of enteric infection in normal mice. J Exp Med. 1974; 139:1189–1203. [PubMed: 4596512]

Chakravarthy MV, Pan Z, Zhu Y, Tordjman K, Schneider JG, Coleman T, Turk J, Semenkovich CF. "New" hepatic fat activates PPARalpha to maintain glucose, lipid, and cholesterol homeostasis. Cell Metab. 2005; 1:309–322. [PubMed: 16054078]

Comelli EM, Simmering R, Faure M, Donnicola D, Mansourian R, Rochat F, Corthesy-Theulaz I, Cherbut C. Multifaceted transcriptional regulation of the murine intestinal mucus layer by endogenous microbiota. Genomics. 2008; 91:70–77. [PubMed: 18035521]

Creely SJ, McTernan PG, Kusminski CM, Fisher M, Da Silva NF, Khanolkar M, Evans M, Harte AL, Kumar S. Lipopolysaccharide activates an innate immune system response in human adipose tissue in obesity and type 2 diabetes. Am J Physiol Endocrinol Metab. 2007; 292:E740–747. [PubMed: 17090751]

Devaraj S, Dasu MR, Park SH, Jialal I. Increased levels of ligands of Toll-like receptors 2 and 4 in type 1 diabetes. Diabetologia. 2009; 52:1665–1668. [PubMed: 19455302]

el Marjou F, Janssen KP, Chang BH, Li M, Hindie V, Chan L, Louvard D, Chambon P, Metzger D, Robine S. Tissue-specific and inducible Cre-mediated recombination in the gut epithelium. Genesis. 2004; 39:186–193. [PubMed: 15282745]

Finnie IA, Dwarakanath AD, Taylor BA, Rhodes JM. Colonic mucin synthesis is increased by sodium butyrate. Gut. 1995; 36:93–99. [PubMed: 7890244]

Fiorentino M, Zadra G, Palescandolo E, Fedele G, Bailey D, Fiore C, Nguyen PL, Migita T, Zamponi R, Di Vizio D, et al. Overexpression of fatty acid synthase is associated with palmitoylation of Wnt1 and cytoplasmic stabilization of beta-catenin in prostate cancer. Lab Invest. 2008; 88:1340–1348. [PubMed: 18838960]

Garrett WS, Gordon JI, Glimcher LH. Homeostasis and inflammation in the intestine. Cell. 2010; 140:859–870. [PubMed: 20303876]

Godl K, Johansson ME, Lidell ME, Morgelin M, Karlsson H, Olson FJ, Gum JR Jr, Kim YS, Hansson GC. The N terminus of the MUC2 mucin forms trimers that are held together within a trypsin-resistant core fragment. J Biol Chem. 2002; 277:47248–47256. [PubMed: 12374796]

Greaves J, Chamberlain LH. DHHC palmitoyl transferases: substrate interactions and (patho)physiology. Trends Biochem Sci. 2011

Guk SM, Lee JH, Kim HJ, Kim WH, Shin EH, Chai JY. CD4+ T-cell-dependent goblet cell proliferation and expulsion of Gymnophalloides seoi from the intestine of C57BL/6 mice. J Parasitol. 2009; 95:581–590. [PubMed: 19061302]

Hasnain SZ, Thornton DJ, Grencis RK. Changes in the mucosal barrier during acute and chronic Trichuris muris infection. Parasite Immunol. 2011; 33:45–55. [PubMed: 21155842]

Heazlewood CK, Cook MC, Eri R, Price GR, Tauro SB, Taupin D, Thornton DJ, Png CW, Crockford TL, Cornall RJ, et al. Aberrant mucin assembly in mice causes endoplasmic reticulum stress and spontaneous inflammation resembling ulcerative colitis. PLoS Med. 2008; 5:e54. [PubMed: 18318598]

Heimerl S, Moehle C, Zahn A, Boettcher A, Stremmel W, Langmann T, Schmitz G. Alterations in intestinal fatty acid metabolism in inflammatory bowel disease. Biochim Biophys Acta. 2006; 1762:341–350. [PubMed: 16439103]

Igarashi S, Kume E, Narita H, Kinoshita M. Food deprivation depletes gastric mucus glycoprotein in streptozotocin-induced diabetic rats. Jpn J Pharmacol. 2000; 84:51–55. [PubMed: 11043453]

Johansson ME, Larsson JM, Hansson GC. The two mucus layers of colon are organized by the MUC2 mucin, whereas the outer layer is a legislator of host-microbial interactions. Proc Natl Acad Sci U S A. 2011; 108(Suppl 1):4659–4665. [PubMed: 20615996]

Johansson ME, Phillipson M, Petersson J, Velcich A, Holm L, Hansson GC. The inner of the two Muc2 mucin-dependent mucus layers in colon is devoid of bacteria. Proc Natl Acad Sci U S A. 2008; 105:15064–15069. [PubMed: 18806221]

Kandori H, Hirayama K, Takeda M, Doi K. Histochemical, lectin-histochemical and morphometrical characteristics of intestinal goblet cells of germfree and conventional mice. Exp Anim. 1996; 45:155–160. [PubMed: 8726140]

Kau AL, Ahern PP, Griffin NW, Goodman AL, Gordon JI. Human nutrition, the gut microbiome and the immune system. Nature. 2011; 474:327–336. [PubMed: 21677749]

Lodhi IJ, Wei X, Semenkovich CF. Lipoexpediency: de novo lipogenesis as a metabolic signal transmitter. Trends Endocrinol Metab. 2011; 22:1–8. [PubMed: 20889351]

Lu P, Burger-van Paassen N, van der Sluis M, Witte-Bouma J, Kerckaert JP, van Goudoever JB, Van Seuningen I, Renes IB. Colonic gene expression patterns of mucin Muc2 knockout mice reveal various phases in colitisdevelopment. Inflamm Bowel Dis. 2011; 17:2047–2057. [PubMed: 21910166]

Macpherson AJ, Harris NL. Interactions between commensal intestinal bacteria and the immune system. Nat Rev Immunol. 2004; 4:478–485. [PubMed: 15173836]

McGuckin MA, Linden SK, Sutton P, Florin TH. Mucin dynamics and enteric pathogens. Nat Rev Microbiol. 2011; 9:265–278. [PubMed: 21407243]

Meddings JB, Jarand J, Urbanski SJ, Hardin J, Gall DG. Increased gastrointestinal permeability is an early lesion in the spontaneously diabetic BB rat. Am J Physiol. 1999; 276:G951–957. [PubMed: 10198339]

Najjar SM, Yang Y, Fernstrom MA, Lee SJ, Deangelis AM, Rjaily GA, Al-Share QY, Dai T, Miller TA, Ratnam S, et al. Insulin acutely decreases hepatic fatty acid synthase activity. Cell Metab. 2005; 2:43–53. [PubMed: 16054098]

Olson TS, Reuter BK, Scott KG, Morris MA, Wang XM, Hancock LN, Burcin TL, Cohn SM, Ernst PB, Cominelli F, et al. The primary defect in experimental ileitis originates from a nonhematopoietic source. J Exp Med. 2006; 203:541–552. [PubMed: 16505137]

Pussinen PJ, Havulinna AS, Lehto M, Sundvall J, Salomaa V. Endotoxemia is associated with an increased risk of incident diabetes. Diabetes Care. 2011; 34:392–397. [PubMed: 21270197]

Rachmilewitz D, Karmeli F, Takabayashi K, Hayashi T, Leider-Trejo L, Lee J, Leoni LM, Raz E. Immunostimulatory DNA ameliorates experimental and spontaneous murine colitis. Gastroenterology. 2002; 122:1428–1441. [PubMed: 11984528]

Remedi MS, Kurata HT, Scott A, Wunderlich FT, Rother E, Kleinridders A, Tong A, Bruning JC, Koster JC, Nichols CG. Secondary consequences of beta cell inexcitability: identification and prevention in a murine model of K(ATP)-induced neonatal diabetes mellitus. Cell Metab. 2009; 9:140–151. [PubMed: 19187772]

Sellin JH, Chang EB. Therapy Insight: gastrointestinal complications of diabetes--pathophysiology and management. Nat Clin Pract Gastroenterol Hepatol. 2008; 5:162–171. [PubMed: 18268523]

Shoelson SE, Lee J, Goldfine AB. Inflammation and insulin resistance. The Journal of clinical investigation. 2006; 116:1793–1801. [PubMed: 16823477]

Turnbaugh PJ, Ley RE, Mahowald MA, Magrini V, Mardis ER, Gordon JI. An obesity-associated gut microbiome with increased capacity for energy harvest. Nature. 2006; 444:1027–1031. [PubMed: 17183312]

Ueno K, Suzuki Y. p260/270 expressed in embryonic abdominal leg cells of Bombyx mori can transfer palmitate to peptides. J Biol Chem. 1997; 272:13519–13526. [PubMed: 9153197]

Vaishnava S, Yamamoto M, Severson KM, Ruhn KA, Yu X, Koren O, Ley R, Wakeland EK, Hooper LV. The antibacterial lectin RegIIIgamma promotes the spatial segregation of microbiota and host in the intestine. Science. 2011; 334:255–258. [PubMed: 21998396]

Valentini L, Wirth EK, Schweizer U, Hengstermann S, Schaper L, Koernicke T, Dietz E, Norman K, Buning C, Winklhofer-Roob BM, et al. Circulating adipokines and the protective effects of

hyperinsulinemia in inflammatory bowel disease. Nutrition. 2009; 25:172–181. [PubMed: 18849144]

van der Flier LG, Clevers H. Stem cells, self-renewal, and differentiation in the intestinal epithelium. Annu Rev Physiol. 2009; 71:241–260. [PubMed: 18808327]

Van Itallie CM, Gambling TM, Carson JL, Anderson JM. Palmitoylation of claudins is required for efficient tight-junction localization. J Cell Sci. 2005; 118:1427–1436. [PubMed: 15769849]

Velcich A, Yang W, Heyer J, Fragale A, Nicholas C, Viani S, Kucherlapati R, Lipkin M, Yang K, Augenlicht L. Colorectal cancer in mice genetically deficient in the mucin Muc2. Science. 2002; 295:1726–1729. [PubMed: 11872843]

Vijay-Kumar M, Aitken JD, Carvalho FA, Cullender TC, Mwangi S, Srinivasan S, Sitaraman SV, Knight R, Ley RE, Gewirtz AT. Metabolic syndrome and altered gut microbiota in mice lacking Toll-like receptor 5. Science. 2010; 328:228–231. [PubMed: 20203013]

Wakil SJ. Fatty acid synthase, a proficient multifunctional enzyme. Biochemistry. 1989; 28:4523–4530. [PubMed: 2669958]

Wan J, Roth AF, Bailey AO, Davis NG. Palmitoylated proteins: purification and identification. Nat Protoc. 2007; 2:1573–1584. [PubMed: 17585299]

Wei X, Schneider JG, Shenouda SM, Lee A, Towler DA, Chakravarthy MV, Vita JA, Semenkovich CF. De novo lipogenesis maintains vascular homeostasis through endothelial nitric-oxide synthase (eNOS) palmitoylation. J Biol Chem. 2011; 286:2933–2945. [PubMed: 21098489]

Wen L, Ley RE, Volchkov PY, Stranges PB, Avanesyan L, Stonebraker AC, Hu C, Wong FS, Szot GL, Bluestone JA, et al. Innate immunity and intestinal microbiota in the development of Type 1 diabetes. Nature. 2008; 455:1109–1113. [PubMed: 18806780]

Wong RH, Sul HS. Insulin signaling in fatty acid and fat synthesis: a transcriptional perspective. Curr Opin Pharmacol. 2010; 10:684–691. [PubMed: 20817607]

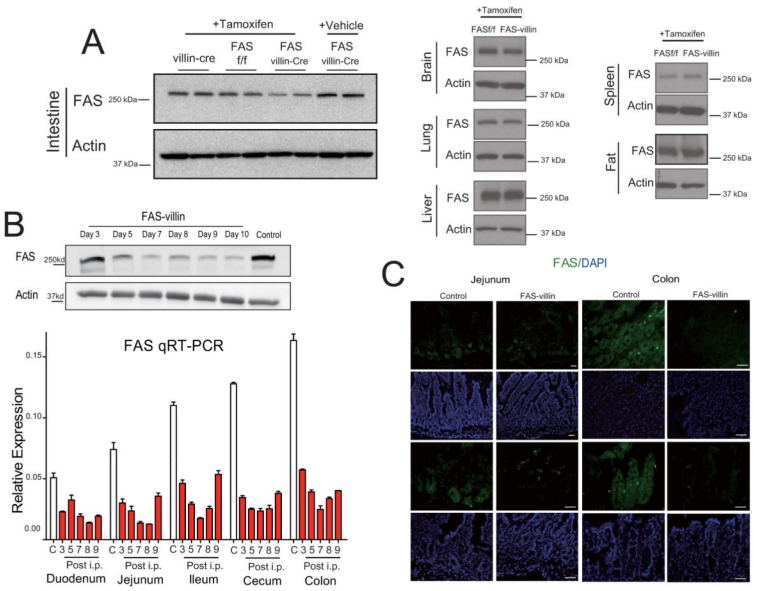

Fig. 1. Intestine-specific deletion of FAS in FAS-villin mice

(**A**) Left panel: Western blotting of FAS and actin in intestinal extracts from tamoxifen-treated villin-Cre mice (without floxed FAS alleles), tamoxifen-treated FAS floxed mice (without villin-Cre), tamoxifen-treated FAS villin-Cre mice (with both floxed FAS alleles and villin-Cre), and from vehicle-treated FAS villin-Cre mice. Right panel: Western blotting of FAS and actin in brain, lung, liver, spleen, and fat recovered from FAS floxed (FASf/f) and FAS-villin (with both floxed FAS alleles and villin-Cre) mice following tamoxifen treatment. (**B**) Upper panel: Western blotting of FAS and actin in colon from FAS-villin animals at various time points after tamoxifen treatment. Bottom panel: q-RT-PCR for intestinal FAS expression in control (C) or FAS-villin mice on days 3–9 after initiation of tamoxifen treatment (n=3 per condition, data presented as mean ± SEM). White indicates control while red indicates tamoxifen treatment. **(C)** Confirmation of intestinal deletion of FAS in FAS-villin mice by immunocytochemistry. The first and third rows show FAS immunostaining (green) in jejunum and colon of control and FAS-villin mice after tamoxifen treatment. The second and fourth rows show DAPI staining (blue). Scale bars: 50 μm.**(A lso see** Fig. S1.)

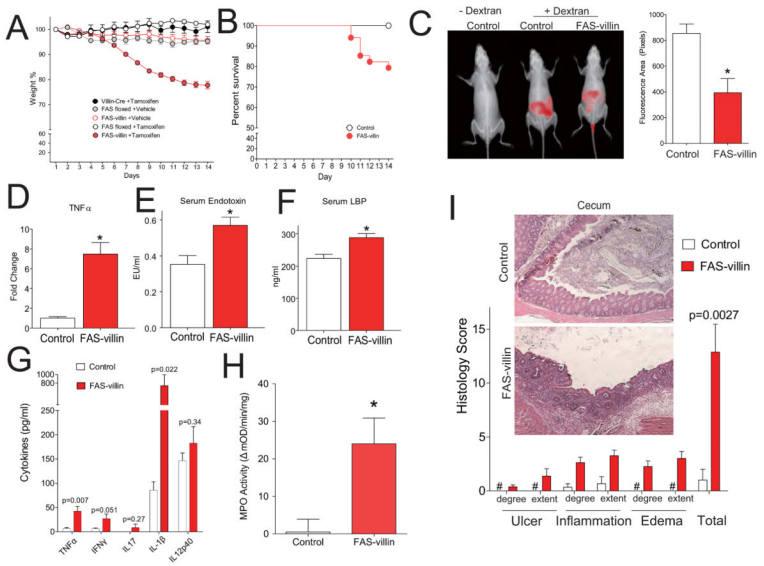

Fig. 2. Intestinal phenotype of FAS-villin mice

(**A**) Mean (± SEM) body weights and (**B**) survival in mice with inducible inactivation of FAS in the gut. Littermates in a series of experiments received injections of Tamoxifen or Vehicle on Days 1–5. FAS-villin (FAS floxed alleles with Villin-Cre) + Tamoxifen, n=46; FAS floxed (without Cre) + Tamoxifen, n=28; FAS-villin + Vehicle, n=7; FAS floxed + Vehicle, n=4, Villin-Cre (without FAS floxed) + Tamoxifen, n=9. For the survival curve, the control symbol represents a composite of all the control groups since there were no deaths in any controls. FAS-villin symbols represent FAS-villin mice treated with tamoxifen on days 1–5. P<0.01 for survival by logrank testing. (**C**) *In vivo* detection of orally administered tracer (10 kDa dextran). Representative imaging is shown on the left and quantitation of fluorescent imaging (presented as pixels detected over a standard area of the abdomen) on the right. *P<0.01 (with data presented as mean ± SEM) by two-tailed unpaired t-test for 12 control and 14 FAS-villin mice. (**D**) TNFα (25 control and 15 FAS-villin mice), (**E**) endotoxin (31 control and 23 FAS-villin mice), and (**F**) LBP (27 mice for each condition) serum levels assayed on day 9 as denoted in **A**. *P<0.01 (with data presented as mean ± SEM) by two-tailed unpaired t-test. (**G**) Levels of secreted cytokines and (**H**) MPO activity from colons (5 control and 4 FAS-villin) 9 days after initiation of tamoxifen injections. Mean values ± SEM are plotted with P values shown or *P<0.05 by two-tailed unpaired t-test. (**I**) Histology scores (mean ± SEM) for the ceca of 6 control and 8 FAS-villin mice. **(Also see** Fig. S2.)

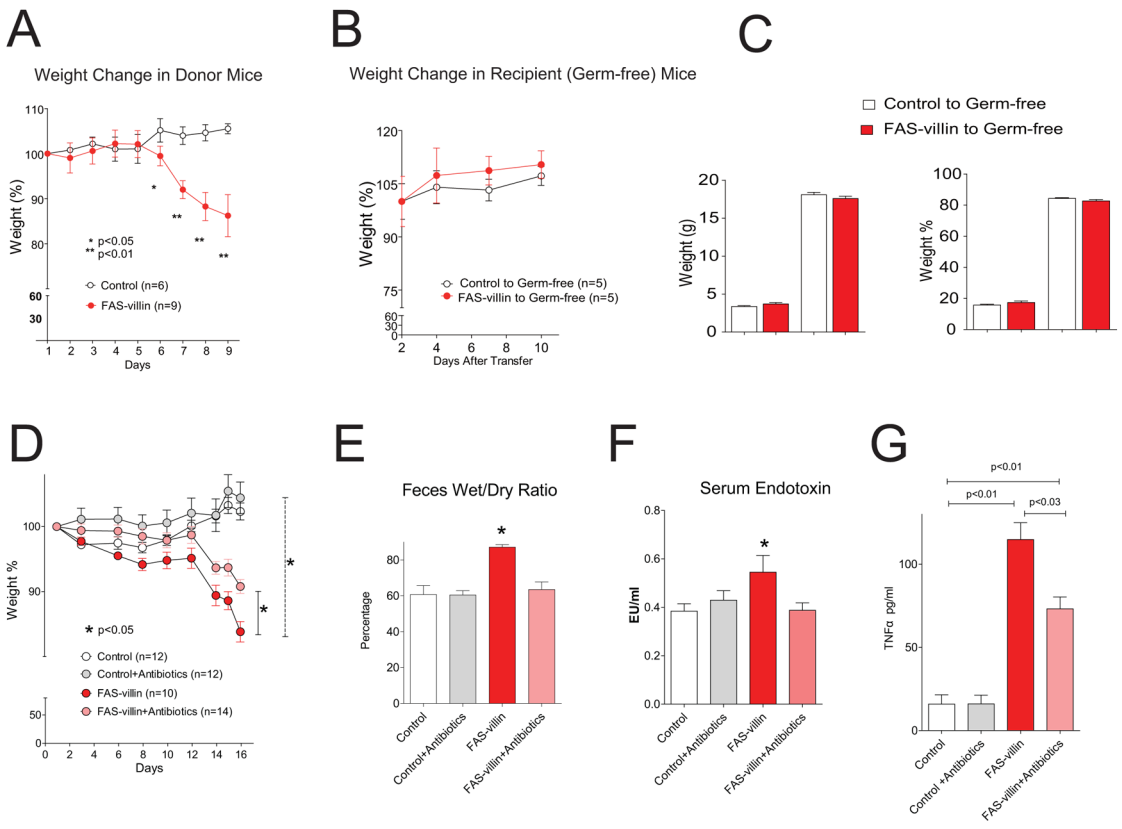

Fig. 3. Microbiota transplantation does not transfer but antibiotic treatment ameliorates the FAS-villin phenotype

(**A**) Weight of donor mice following initiation of tamoxifen treatment on day 1. (**B**) Weight of recipient germ-free mice. (**C**) Body composition of recipient germ-free mice. (**D**) Body weight, (**E**) feces wet/dry ratio, (**F**) serum endotoxin, and (**G**) serum TNFα in control and FAS-villin mice with and without daily antibiotic treatment. P values are shown or *P<0.05. Data are presented as mean ± SEM. **(Also see** Table S1.)

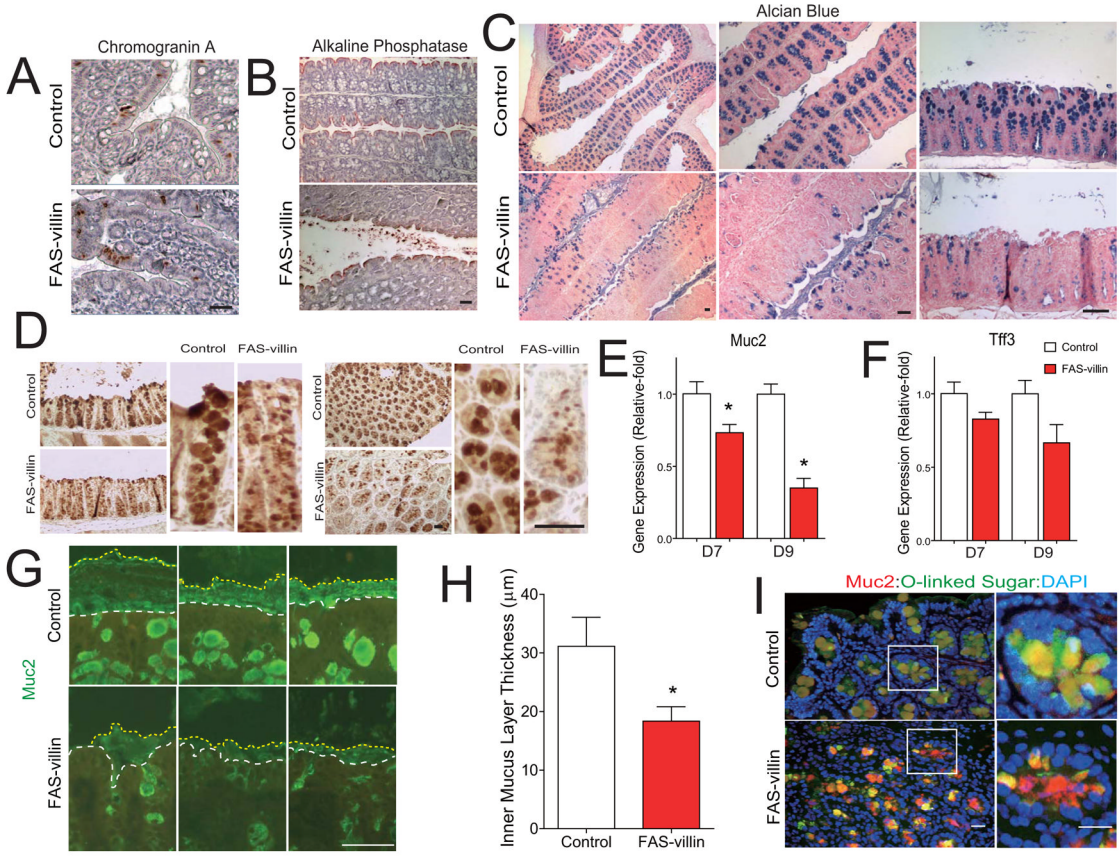

Fig. 4. Muc2 levels are reduced and the inner mucus layer disrupted in the colons of FAS-villin mice

(**A**) Staining for chromogranin A (which detects most enteroendocrine cells) and (**B**) Alkaline phosphatase (biomarker of the enterocytic lineage) in colons of control (FAS floxed animals without Cre treated with tamoxifen) or FAS-villin (FAS floxed animals with villin-Cre treated with tamoxifen) mice. (**C**) Alcian blue staining (to detect goblet cells) in mouse colon. (**D**) Muc2 immunostaining in mouse colon. (**E**) mRNA levels for Muc2 and (**F**) Tff3 in mouse colon at days 7 and 9 as denoted in Fig. 2A (n=5 per condition; mean values ± SEM are plotted; *P<0.05 by t-test). (**G**) Disruption of the colonic mucus layer in FAS-villin mice detected by Muc2 immunocytochemistry. The white dashed lines denote the epithelial cell surface while the yellow dashed lines indicate the luminal border of the inner mucus layer. (**H**) Average thickness of the inner mucus layer measured at the proximal colon. Measurements were made perpendicular to the inner mucus layer at 5–7 different sites for each colon. Data represent thickness determinations for 5 mice per condition. Mean values ± SEM are plotted. *P<0.05 (t-test). (**I**) Merged images of Muc2 (red) and DBA (green) staining in the colons of control and FAS-villin mice. Scale bar: 50 μm. (**Also see** Fig. S3)

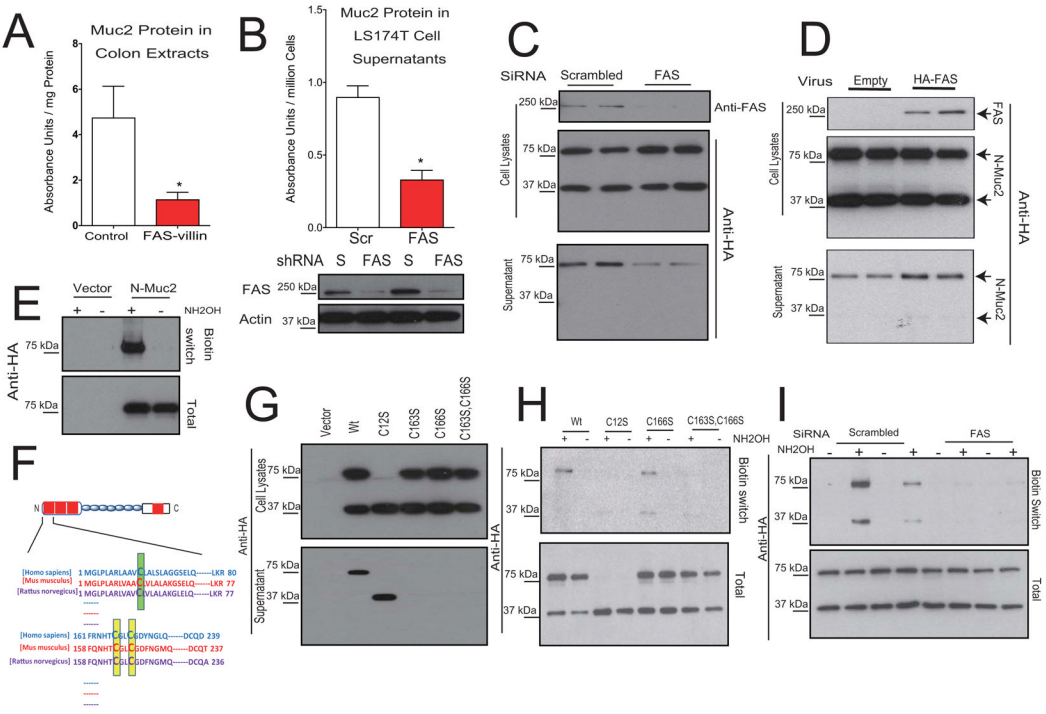

Fig. 5. FAS-dependent S-palmitoylation is required for normal Muc2 secretion

(**A**) Muc2 protein content assayed by ELISA (mean ± SEM) in colon extracts from mice at day 7 as denoted in Fig. 2A. (**B**) Muc2 protein content (mean ± SEM) secreted from LS174T cells following lentivirus-mediated shRNA knockdown of FAS. Verification of the knockdown is shown by Western blotting in the bottom panels. (**C**) The HA-tagged Muc2 N-terminus (N-Muc2) was expressed in COS7 cells, which were treated with a control (scrambled) or FAS-specific siRNA. The top panel shows Western blotting with an antibody to FAS, and the bottom panels blotting with an anti-HA antibody. (**D**) HA-tagged FAS was overexpressed in COS cells using a retrovirus, then N-Muc2 was expressed in the same cells. The top panel verifies expression of the tagged FAS. The bottom panels show Western blotting of N-Muc2, distinguished from FAS by differences in protein size. (**E**) Biotin switch assay demonstrates S-palmitoylation of N-Muc2 by detecting a biotin moiety that is hydroxylamine (NH_2OH)-dependent. (**F**) Sequence alignment of human, mouse and rat N-Muc2 with the conserved Cys12 residue (mouse) indicated in green and the conserved Cys163 and Cys166 residues (mouse) indicated in yellow. (**G**) Western blotting of lysates or culture supernatants for N-Muc2 mutants. (**H**) Biotin switch assay using wild type N-Muc2 and N-Muc2 mutants. (**I**) Biotin switch assay for N-Muc2 S-palmitoylation in control (scrambled) and FAS knockdown cells. **(Also see** Fig. S4.)

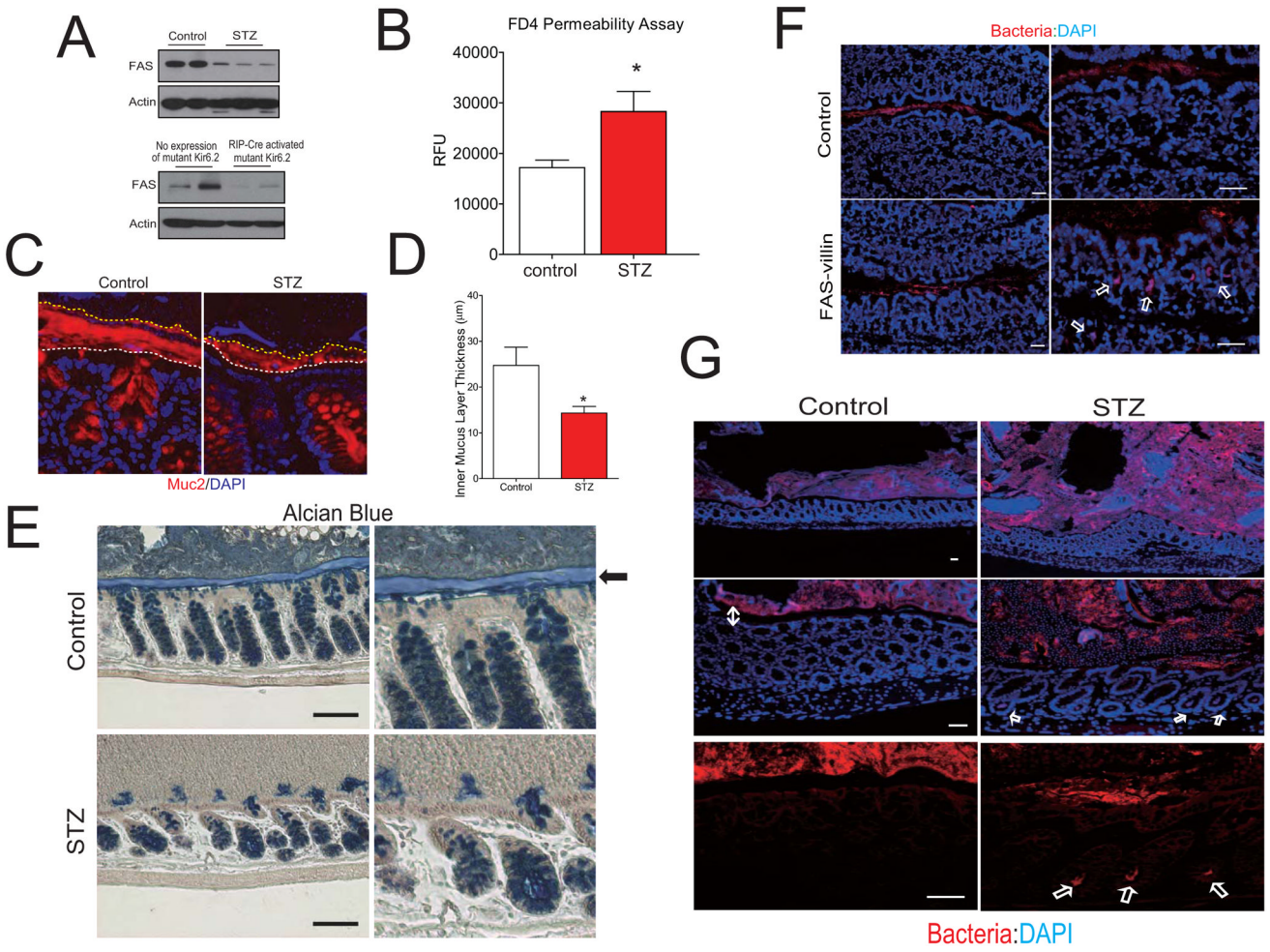

Fig. 6. Mice with experimental diabetes have phenotypic features that resemble those of mice with conditional deletion of FAS in the gut

(**A**) Western blotting for FAS and actin in colon extracts from diabetic mice. For panels on the top, streptozotocin (STZ) or vehicle (control) was injected into C57BL/6 male mice. For panels on the bottom, non-diabetic mice with no expression of a mutant Kir6.2 and hyperglycemic mice with overexpression of a mutant Kir6.2 induced by RIP-Cre were studied. (**B**) Serum fluorescence (expressed as relative fluorescence units or RFUs, mean ± SEM) following gavage of mice with FITC-dextran (4 kDa). (**C**) Detection of disruption of the inner mucus layer by anti-Muc2 staining in STZ-treated mice. The white dashed lines mark the epithelial cell surface while the yellow dashed lines identify the luminal border of the inner mucus layer. (**D**) Colons were fixed in methanol-Carnoy fixative without disruption of fecal contents following by determination of the thickness of the inner mucus layer. Measurements were made perpendicular to the inner mucus layer at 5–7 different sites for each colon. Data represent thickness determinations for 6–7 mice per condition. Mean values ± SEM are plotted. *P<0.05 (t-test). (**E**) Alcian blue staining for mucus-producing goblet cells in the colons of control or STZ mice. The arrow indicates the inner adherent mucus layer. (**F**) Fluorescent *in situ* hybridization for bacteria (red) in colon from wild type and FAS-villin mice. Nuclei are stained with DAPI. As expected, bacteria are detected by red color in the lumen, but arrows denote bacterial penetration of the epithelium in FAS-villin colon. (**G**) Fluorescent hybridization of bacteria in colon from control or STZ mice.

The double-headed arrow identifies a clear space separating bacteria and epithelium in control mice. Single arrows denote bacterial penetration into crypts in STZ mice. Scale bars: 50μm.**(A lso see** Fig. S5.)

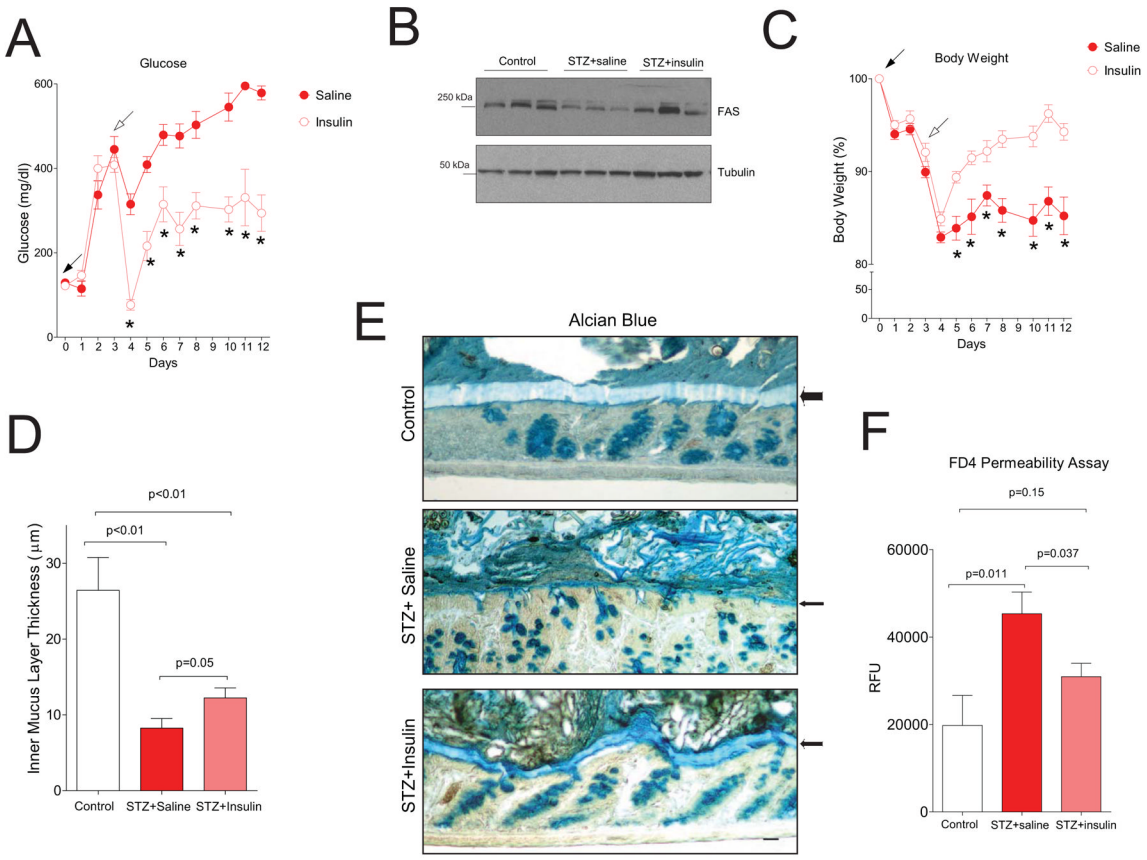

Fig. 7. Correction of the intestinal permeability defect by insulin in experimental diabetes

(**A**) Glucose levels in mice injected with STZ on day 0 (solid arrow), then implanted with pumps delivering saline or insulin (7 mice per condition) on day 3 (open arrow). (**B**) Western blotting of FAS protein in colons of mice at day 12. (**C**) Body weight of treated mice. (**D**) Inner mucus layer thickness for control (n=4), saline-treated diabetic mice (STZ +saline, n=7), and insulin-treated diabetic mice (STZ+insulin, n=7). (**E**) Alcian blue images from the animals shown in panel D. (**F**) Intestinal permeability assay of animals after gavage with FD4 (n=5 for non-diabetic controls and n=7 for each diabetic group). P values are shown or *P<0.05 (data presented as mean ± SEM).